Demonstration of Single-Crystal Self-Seeded Two-Color X-Ray Free-Electron Lasers/article-title>

A. A. Lutman, F.-J Decker, J. Arthur, M. Chollet, Y. Feng, J. Hastings, Z. Huang, H.-D. Nuhn, A. Marinelli, J. L. Turner, S. Wakatsuki, J. Welch, and D. Zhu

Demonstration of Single-Crystal Self-Seeded Two-Color X-Ray Free-Electron Lasers

A.A. Lutman,* F.-J Decker,† J. Arthur, M. Chollet, Y. Feng, J. Hastings, Z. Huang, H. Lemke, H.-D. Nuhn, A. Marinelli, J.L. Turner, S. Wakatsuki, J. Welch, and D. Zhu

SLAC National Accelerator Laboratory, Menlo Park, California 94025, USA
(Dated: November 19, 2014)

A scheme for generating two simultaneous hard X-ray free-electron laser pulses with a controllable difference in photon energy is described, and demonstrated using the self-seeding setup at the Linac Coherent Light Source (LCLS). The scheme takes advantage of the existing LCLS equipment which allows two independent rotations of the self-seeding diamond crystal. The two degrees of freedom are used to select two nearby crystal reflections, causing two wavelengths to be present in the forward transmitted seeding X-ray pulse. The FEL system must support amplification at both desired wavelengths.

The Linac Coherent Light Source (LCLS) is the worlds first hard X-ray (HXR) Free Electron Laser (FEL), having begun operation in 2009 [1]. Another hard X-ray FEL, SACLA, has recently begun operation in Japan[2]. Two soft X-ray facilities are also in operation: FLASH[3] in Germany, and FERMI[4, 5] in Italy. All of these new FEL facilities feature coherent amplification of a relatively narrow-bandwidth X-ray pulse, delivering to the users photon beams with unprecedented properties such as ultra-short pulse duration ranging from a few to hundreds of femtoseconds, ultra-high peak brightness, and nearly full spatial coherence in the transverse directions. The initial success of these X-ray FEL facilities has already sparked interest in expanding their capabilities so as to provide greater control over the temporal and spectral properties of the FEL radiation. For example, some experimental techniques such as pump-probe with two different colors or multi-wave mixing require two pulses of slightly different color, either simultaneously or with controlled delay. It is also desirable to control the bandwidth and temporal coherence of the intense FEL pulses. Both narrow-bandwidth (seeded FEL) operation and two-color FEL operation have been demonstrated separately. This Letter describes a new technique which combines two-color and seeded FEL operation at hard X-ray wavelengths.

Though X-ray FEL machines have been used to produce two-color beams in both the hard and soft X-ray regions [6–8], so far they have always relied on the SASE mode, amplifying noise in the initial electron pulse. Two colors were generated by tuning some undulator segments to one k value and some to another. Seeded two-color FEL operation, with radiation properties determined by the seed pulses, has previously not been tried in the X-ray region, though it has been demonstrated in the extreme UV regime, using a chirped external seed laser [9, 10] or two external seed lasers with different wavelengths [11].

In the hard X-ray wavelength regime, many two-color experiments require narrow bandwidth and wavelength stability. For instance, in the determination of protein structures, the spiky nature and shot-to-shot variation of the SASE photon energy spectra have so far prevented extraction of intensity measurements at an accuracy needed for de novo phase determination. While attempts have been made to develop methods which incorporate photon energy-spectrum measurements into data analysis, it would be more advantageous to have X-ray pulses with smoother and better-defined photon energy spectra. Multi-wavelength anomalous diffraction (MAD) is generally used at synchrotron sources for accurate and model-bias-free phase determination[12], by collecting data at 2 or 3 wavelengths, one at a time and by using the same sample crystal. At XFELs, since the crystal is destroyed after each pulse, one needs two-color pulses which arrive at the same time, allowing two diffraction patterns to be collected simultaneously. Maximization of the anomalous signal would require a difference between the two colors of about 1 eV for typical heavy atoms, but the need of differentiating the diffraction spots on the detector typically requires a wider color separation.

Creating two simultaneous narrow-band FEL beams could also enhance the capability of an FEL facility to multiplex its source, allowing two single-color experiments to take place simultaneously and independently. This would help to increase the efficiency of the facility operation and allow more experiments to take place.

In this Letter we describe a novel technique for generating two-color self-seeded beams in the hard X-ray regime using a single monochromatizing crystal, and more in general allowing us to double the number of self-seeded beams in respect to the standard operation. We present also the experimental demonstration of the scheme.

The Linac Coherent Light Source (LCLS) undulator section layout [1], after modifications introduced to operate in hard X-ray self-seeded mode [13, 14], consists of two undulator sections separated by a magnetic chicane with a diamond crystal monochromator (see Figure 1).

The X-ray seed in the LCLS approach is originated from a SASE FEL photon pulse developed in the first undulator section, reaching GW power levels, before saturation. In the chicane section the electron beam is diverted while the X-ray pulse hits the diamond crystal, where a narrow-band portion of it can be diffracted (in either Bragg reflection or Laue transmission geometry). The
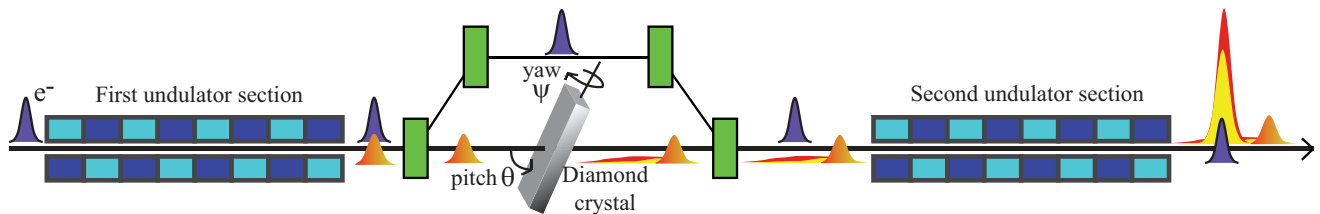
FIG. 1. Single-crystal self-seeding scheme at LCLS. In the first undulator section a self-amplified spontaneous emission (SASE) photon pulse is generated. This photon pulse diffracts from a diamond crystal. The diffracted bandwidth is at least an order of magnitude smaller than the SASE bandwidth. The diffracted beam exits at some angle to the incident beam, and is discarded. The undiffracted, transmitted pulse consists of a wide-bandwidth short pulse followed by a relatively weak narrow-bandwidth tail. The electron pulse is delayed by the magnetic chicane to overlap spatially with the narrow-bandwidth tail of the X-ray pulse in the second undulator section. The narrow-bandwidth tail, with long temporal coherence length, seeds FEL amplification in the second undulator section, generating a narrow-band intense X-ray output.
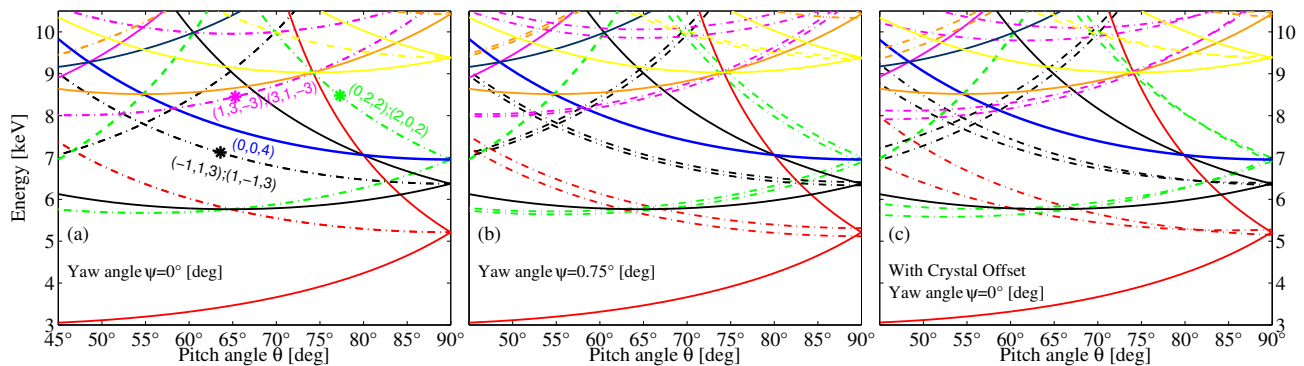

FIG. 2. Photon energy values at which diffraction occurs in a diamond crystal, as a function of the pitch angle θ for fixed values of yaw angle ψ. Each curve corresponds to reflection from a different set of crystallographic planes. (a) Yaw angle $\psi = 0°$. Stars represent demonstrated two-color working points. (b) Yaw angle $\psi = 0.75°$. Different colors represent planes with different $h^2 + k^2 + l^2$ value. Dash-dotted lines are double-lines (two sets of crystal planes excited) that are superposed for $\psi = 0°$ and can be separated with a non-zero yaw angle. (c) Correcting for the small crystal orientation offset deduced from experimental measurements of the energies as a function of (θ, ψ) values.

diffracted X-rays are not used. The undiffracted X-ray pulse transmitted through the diamond crystal consists of a wide-bandwidth short pulse (similar in duration and bandwidth to the incident SASE pulse) followed by a relatively weak narrow-bandwidth tail (a result of the very narrow bandwidth of the diffraction). The short, diverted electron pulse is delayed just long enough so that in the second undulator section it overlaps spatially with the narrow-bandwidth tail of the X-ray pulse, which serves to seed FEL amplification yielding an intense narrow-bandwidth X-ray output. Thus the seeded XFEL output depends on the diffraction process in the diamond crystal, which depends primarily on the crystal orientation with respect to the incident beam direction. Rigorous treatment of both Bragg and Laue geometries can be found in [15, 16]. The diamond crystal orientation can be controlled by means of a pitch rotational stage, with a pitch angle θ in the range $45° \leq \theta \leq 90°$, and a yaw rotational stage, with a yaw angle ψ in the range $-2.5° \leq \psi \leq 2.5°$. The angle θ is the glancing angle

between the beam propagation direction and the planes of the (0,0,4) reflection. The pitch stage has rotation axis orthogonal to the beam propagation direction and parallel to the floor, while the yaw stage rotates on top of the pitch stage and has an axis lying parallel to the beam propagation direction when $\theta = 0°$. The diamond crystal sits on these stages with its (-1,1,0) direction parallel to the θ axis and its (1,1,0) direction parallel to the ψ axis (the effects of a slight misalignment are discussed below). It is possible to excite two (or more) reflections simultaneously within the bandwidth of the SASE seed source. In this case the narrow-bandwidth tail of the X-ray pulse transmitted through the diamond contains more than one energy, and can seed an FEL output containing more than one energy. Each energy present in the narrow-band tail can be determined by applying subsequently the pitch and yaw rotation to the diamond crys-

tal and then using Bragg's law:

$$E=\frac{ch_p\left(h^2+k^2+l^2\right)}{a_0\left|\sqrt{2}\left[(h+k)\cos\theta+(k-h)\sin\theta\sin\psi\right]-2l\sin\theta\cos\psi\right|},$$

$$(1)$$

where c is the velocity of light in the vacuum, h_p is the Planck constant and a_0 is the crystal lattice parameter. h, k, and l are the Miller indices of a particular set of crystal planes. For the diamond crystal, $a_0 = 0.35668$ nm. Figure 2 shows the loci of all allowed diamond reflections with energies in the range $3 - 10.5$ keV as a function of the angle θ, for fixed angles ψ. Different colors represent different allowed reflections. Of particular interest for the two-color self-seeded operation are the dash-dotted lines. When the yaw angle is set to $0°$, as in Fig. 2(a), those lines represent pairs of reflections which track together, producing identical energies for any θ. When the yaw angle assumes small non-zero values, as in Fig. 2(b) where $\psi = 0.75°$, these two lines separate slightly in energy. These are the most suitable crystal reflections for the two-color self-seeding scheme because they allow easy control of both the central energy and the separation between the two colors. Such double lines can be found for energies down to 5.2 keV for the diamond crystal. From Eq. 1, the double lines are defined as those in the form (h_1,k_1,l_1) and (h_2,k_2,l_2) with $l_1 = l_2$ and $h_1 = k_2$ and $k_1 = h_2$ and $h_1 \neq k_1$. For small values of the yaw angle, the central energy can be approximated with the one for $\psi = 0°$ as

$$\bar{E} \approx \frac{ch_p\left(h^2+k^2+l^2\right)}{a_0\left|\sqrt{2}\left[(h+k)\cos\theta\right]-2l\sin\theta\right|}\qquad(2)$$

and the difference between the energies can be approximated by

$$\Delta E \approx \left|\frac{ch_p\sqrt{2}(k-h)(h^2+k^2+l^2)\sin\theta}{a_0\left[(h+k)\cos\theta-\sqrt{2}l\sin\theta\right]^2}\,\psi\right|\qquad(3)$$

Experimental measurements of the self-seeded energies as a function of the diamond crystal angles showed that the initial orientation of the crystal was slightly different from the design value. Figure 2(c) has been calculated taking this offset into account. As a consequence of the offset, double lines are separated even for $\psi = 0°$.

In order for the two-color seeding scheme to work effectively, both colors must fall within the FEL amplification bandwidth both in the first and in the second undulator sections, limiting the achievable separation between them. With the standard electron beam used for hard X-ray operation, this constraint limits the achievable separation to $\sim 0.2\%$ of the photon energy at LCLS.

The single-crystal two-color self-seeded FEL was demonstrated at LCLS by generating a two-color beam with the reflections (1,3,-3) and (3,1,-3). The electron pulse charge was 150 pC, the average bunch length was 58 fs and the delay of the magnetic chicane was set to 30 fs, while the maximum delay allowed by the existing chicane is 40 fs. The pitch angle was set to $65.28°$ and the resulting photon beam energy was close to 8.43 keV. Figure 3 shows 111 consecutive shots average spectra collected by a bent crystal spectrometer [17], while scanning the yaw angle from $1.47°$ to $1.53°$ in steps of $0.02°$. The average pulse energy was $\sim 400\,\mu$J. The separation between the two colors can be controlled more finely by manipulating the yaw angle in smaller steps. Chicane delay was set by scanning its value to maximize the intensity in the colors bandwidth, this setting yields a large SASE pedestal as in Fig. 3, deriving mainly from the wide-bandwidth head pulse amplified in the second undulator section due to its partial overlap with the electron beam.

A transverse shift of the forward diffracted wake is predicted by [16] and could lead to an increase of the transverse size of the beam from single color to two double color operation. In our experiment we haven't seen two different transverse spots for the two colors, nor a broadening of the spot size.

Correlations between the two color intensities were studied using a set of 3500 shots, recorded using the (0,2,2) and (2,0,2) reflections at 8.43 keV, with the angles $(\theta,\psi) = (77.26°, 0.27°)$; the electron bunch duration was 50 fs. Figure 4(a) shows the average spectrum of the collected shots, whose average pulse energy was $412\,\mu$J. Figure 4(b) shows the correlation between the intensities of the two colors in a 1 eV bandwidth around the peak of each color. The experimental set presents a slight positive correlation between the two intensities, with a coefficient of correlation of 0.1. Different tendencies can be identified to explain the intensity correlation between the colors within a single shot. Negative correlation is provided by the competition for the same electron beam, because if one color reaches saturation the degradation of the electron beam quality slows the amplification for the other color. Also the electron beam energy jitter has an impact on the correlation, especially when it yields a SASE central wavelength jitter comparable with the SASE bandwidth or larger. When the separation between the two colors is large, the electron beam energy will better support either the growth of one color or the other leading to negative correlation, while when the separation between the two colors is small, one particular electron beam energy tends either to support or prevent the growth of both. 4(c) depicts the situation for our experimental data, in which the separation between the two colors is small in respect to the energy jitter. Figure 4(d) shows an histogram of the event rate as function of the difference between the intensities of the two colors.

A larger separation between the two colors can be achieved by using an electron beam with two different energy levels, thereby increasing the FEL amplification bandwidth. This has been experimentally demonstrated by introducing a strong time-correlated energy chirp on the electron beam by using the X-band linearizer, re-
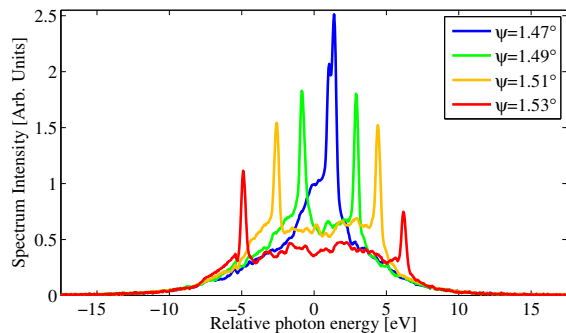
FIG. 3. Average spectra from 111 consecutive shots for single-crystal two-color self-seeded beams with photon energy close to 8.43 keV. The pitch angle was fixed to $\theta = 65.28°$. (blue) yaw angle $\psi = 1.47°$. (green) $\psi = 1.49°$. (orange) $\psi = 1.51°$. (red) $\psi = 1.53°$. The used reflection planes were (-1,-3,3) and (-3,-1,3). The average spectra are shown without post-processing, including the SASE pre-pulse. The plateau between the two narrow colors is mainly due to the wide-bandwidth head part amplified in the second undulator section.
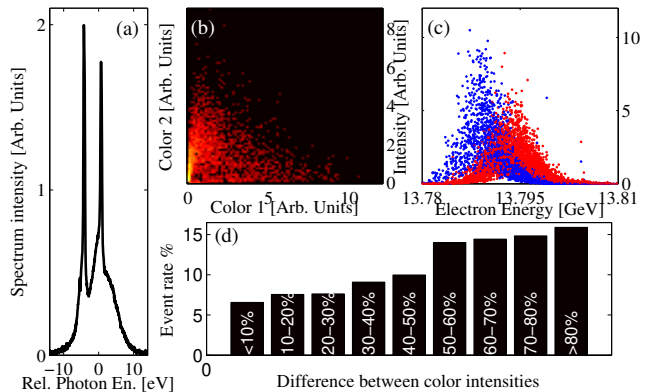

FIG. 4. Single-crystal two-color self seeding experimental results for 3500 consecutive shots. Photon energy was close to 8.43 keV, the reflections used were (2,0,2) and (0,2,2). (a) Average spectrum. (b) Correlation between the first and second color intensities in a 1 eV bandwidth around each color average peak energy. (c) Single-shot intensities in a 1 eV bandwidth for both colors vs electron beam energy, (blue) color 1; (red) color 2. (d) Histogram of the events rate as function of the difference between the intensities of the two colors.
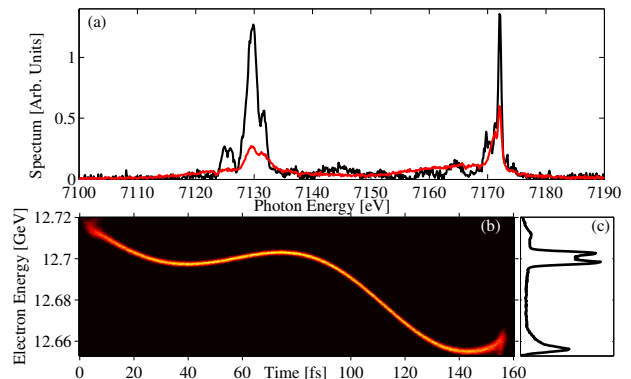
sulting in a large separation at the iron absorption edge with one spectral line at 7130 eV and a second line at 7173 eV. Figure 5(a) shows a 120 μJ single-shot the and average spectrum with a separation between the two colors of ∼ 0.6%. The two-color amplification bandwidth needed for such separation is granted by the two energy levels present in the electron beam phase space. Figure 5(b) shows a simulated electron beam phase space calculated with LiTrack [18], and reveals a drawback of the phase space manipulation with the linearizer: the two energy levels seen in the profile in Fig. 5(c) are temporally separated by ∼ 70 fs. This means that the colors, are also temporally separated by about ∼ 70 fs. Wider energy separations, on the order of ∼1%, and independent tunability of the time-delay between the two colors can be supported by the two-bunch scheme where two electron bunches are accelerated in the same radio-frequency bucket, demonstrated in the optical regime [19], and proposed by A. Marinelli in the x-rays[20].

Multicolor operation with more than two colors could also be achieved by arranging the crystal so that more than two lines in Fig. 2 are found within the FEL amplification bandwidth. However, with only two degrees of freedom available to set the diamond crystal orientation, it is not possible to choose all the wavelengths independently. By implementing the scheme to generate two-color beams, which uses a series of monochromatizing crystals[21], and adding independent pitch and yaw control one could set up to four desired wavelengths.

Two-color scans can be performed by moving each color independently by changing both crystal angles at the same time. During the scan both seeded wavelengths have to stay within the FEL amplification bandwidth.

FIG. 5. (a) two-color self-seeded spectrum obtained by using the (-1,1,3) and (1,-1,3) reflections, single-shot (black), average on 100 shots (red). The two color lines are separated by 43 eV (∼ 0.6%) which is wider than the SASE bandwidth for the normal LCLS operation. The pulse energy for the shot was 120μJ. (b) LiTrack simulated phase space obtained by manipulating the X-band linearizer. (c) Simulated two energy levels electron beam energy profile.

* aal@slac.stanford.edu
† decker@slac.stanford.edu

[1] P. Emma *et al.*, Nat. Photon. **4**, 641 (2009).
[2] T. Ishikawa *et al.*, Nat. Photon. **6**, 540 (2012).
[3] W. Ackermann *et al.*, Nat. Photon. **1**, 336 (2007).
[4] E. Allaria *et al.*, Nat. Photon. **6**, 699 (2012).
[5] E. Allaria *et al.*, Nat. Photon. **7**, 913 (2013).
[6] A. A. Lutman, R. Coffee, Y. Ding, Z. Huang, J. Krzywinski, T. Maxwell, M. Messerschmidt, and H.-D. Nuhn, Phys. Rev. Lett. **110**, 134801 (2013).
[7] A. Marinelli, A. A. Lutman, J. Wu, Y. Ding, J. Krzywinski, H.-D. Nuhn, Y. Feng, R. N. Coffee, and C. Pellegrini, Phys. Rev. Lett. **111**, 134801 (2013).
[8] T. Hara *et al.*, Nature Communications **4** (2013), 10.1038/ncomms3919.
[9] G. De Ninno, B. Mahieu, E. Allaria, L. Giannessi, and S. Spampinati, Phys. Rev. Lett. **110**, 064801 (2013).
[10] B. Mahieu and Others, Optics Express **21**, 22728 (2013).
[11] E. Allaria *et al.*, Nature Communications **4** (2013), 10.1038/ncomms3476.
[12] W. A. Hendrickson and C. M. Ogata, in *Macromolecular Crystallography Part A*, Methods in Enzymology, Vol. 276, edited by J. Charles W. Carter (Academic Press, 1997) pp. 494 – 523.
[13] J. Amman *et al.*, Nat. Photon. **6**, 693 (2012).
[14] G. Geloni, K. Vitali, and E. Saldin, Journal of Modern Optics **58:16**, 1391 (2011).
[15] R. R. Lindberg and Y. V. Shvyd'ko, Phys. Rev. ST Accel. Beams **15**, 050706 (2012).
[16] Y. Shvyd'ko and R. Lindberg, Phys. Rev. ST Accel. Beams **15**, 100702 (2012).
[17] D. Zhu *et al.*, Appl. Phys. Lett. **101**, 034103 (2012).
[18] K. Bane and P. Emma, *SLAC-PUB-11035, LiTrack: A Fast longitudinal phase space tracking code with graphical user interface*, Tech. Rep. (2005).
[19] V. Petrillo *et al.*, Phys. Rev. Lett. **111**, 114802 (2013).
[20] A. Marinelli, Private Communication (2014).
[21] G. Geloni, V. Kocharyan, and E. Saldin, Optics Communications **284**, 3348 (2011).